THE JOURNAL OF BIOLOGICAL CHEMISTRY VOL. 286, NO. 18, pp. 15854–15861, May 6, 2011
Printed in the U.S.A.

Inhibition of Ebola Virus Entry by a C-peptide Targeted to Endosomes*[S]

Received for publication, November 26, 2010, and in revised form, March 15, 2011 Published, JBC Papers in Press, March 16, 2011, DOI 10.1074/jbc.M110.207084

Emily Happy Miller[‡1,2], Joseph S. Harrison[§1,3], Sheli R. Radoshitzky[¶], Chelsea D. Higgins[§], Xiaoli Chi[¶], Lian Dong[¶], Jens H. Kuhn[‖], Sina Bavari[¶], Jonathan R. Lai[§4], and Kartik Chandran[‡5]**

*From the Departments of [‡]Microbiology and Immunology and [§]Biochemistry, Albert Einstein College of Medicine, Bronx, New York 10461, the [¶]United States Army Medical Research Institute of Infectious Diseases, Fort Detrick, and the [‖]Integrated Research Facility at Fort Detrick, NIAID, National Institutes of Health, Frederick, Maryland 21702, and **Tunnell Consulting, Incorporated, King of Prussia, Pennsylvania 19406*

Ebola virus (EboV) and Marburg virus (MarV) (filoviruses) are the causative agents of severe hemorrhagic fever. Infection begins with uptake of particles into cellular endosomes, where the viral envelope glycoprotein (GP) catalyzes fusion between the viral and host cell membranes. This fusion event is thought to involve conformational rearrangements of the transmembrane subunit (GP2) of the envelope spike that ultimately result in formation of a six-helix bundle by the N- and C-terminal heptad repeat (NHR and CHR, respectively) regions of GP2. Infection by other viruses employing similar viral entry mechanisms (such as HIV-1 and severe acute respiratory syndrome coronavirus) can be inhibited with synthetic peptides corresponding to the native CHR sequence ("C-peptides"). However, previously reported EboV C-peptides have shown weak or insignificant antiviral activity. To determine whether the activity of a C-peptide could be improved by increasing its intracellular concentration, we prepared an EboV C-peptide conjugated to the arginine-rich sequence from HIV-1 Tat, which is known to accumulate in endosomes. We found that this peptide specifically inhibited viral entry mediated by filovirus GP proteins and infection by authentic filoviruses. We determined that antiviral activity was dependent on both the Tat sequence and the native EboV CHR sequence. Mechanistic studies suggested that the peptide acts by blocking a membrane fusion intermediate.

Ebola virus (EboV)[6] and Marburg virus (MarV) are members of the *Filoviridae* family of non-segmented negative-strand RNA viruses that produce filamentous enveloped particles (1, 2). Several filoviruses cause rapidly progressing hemorrhagic fevers, with human case-fatality rates exceeding 90% in larger outbreaks (1, 3). There are currently no vaccines or antivirals approved in the United States to treat filovirus infections. The infectious filovirus particle possesses a single membrane glycoprotein (GP), which is necessary and sufficient to mediate entry into host cells (4, 5). During viral assembly, GP is cleaved into two subunits (GP1 and GP2) by furin to produce the mature envelope spike that consists of a trimer of disulfide-linked GP1-GP2 heterodimers (6–9). The surface subunit, GP1, mediates viral attachment and regulates the conformation of the membrane fusion subunit, GP2 (7, 10–16). Filovirus GP proteins are categorized into the structurally defined "class I" viral membrane fusion glycoproteins that have a high α-helical content (17–19). Similar to the prototypic class I fusion proteins of HIV-1 and influenza A virus, GP2 contains a hydrophobic fusion peptide near its N terminus, followed by N- and C-terminal heptad repeat (NHR and CHR, respectively) sequences and the transmembrane domain (7, 17, 20–24).

A current model for filovirus entry into cells based on experimental evidence and analogy to the HIV-1 and influenza A virus entry mechanisms is schematically depicted in Fig. 1 (17, 20, 25). Following cell attachment, virus particles are internalized into endosomes. Here, the host endosomal cysteine proteases cathepsin L and cathepsin B are proposed to cleave GP1 to remove a large C-terminal region (26, 27). This proteolytic remodeling (resulting in a "cleaved" GP intermediate) exposes a putative receptor-binding site in GP1 (7, 11, 16, 28). Cleavage of GP1 by cathepsin L/cathepsin B is also thought to destabilize the pre-fusion conformation of the GP1-GP2 complex, promoting deployment of the GP2 fusion machine (29).[7] Next, GP2 is released from its pre-fusion conformation, presumably by an unknown trigger, and drives membrane fusion by undergoing a series of large-scale conformational changes (7, 17, 20, 22, 23, 25). The three NHRs are thought to rearrange to form a long

* This work was supported, in whole or in part, by National Institutes of Health Grants R01 AI088027 (to K. C.) and R01 AI090249 (to J. R. L.). This work was also supported by the Albert Einstein College of Medicine, the Arnold and Mabel Beckman Foundation Young Investigators Program (to J. R. L.), and Joint Science and Technology Office Transformational Medical Technologies Proposal TMTI0048_09_RD_T and Defense Threat Reduction Agency Proposal 4.10022_08_RD_B (to S. B.). J. H. K. performed this work as an employee of Tunnell Consulting, Inc., a subcontractor to Battelle Memorial Institute under its prime contract with NIAID, under Contract No. HHSN272200200016I.

[S] The on-line version of this article (available at http://www.jbc.org) contains supplemental "Results" and Figs. S1–S4.

[1] Both authors contributed equally to this work.

[2] Additionally supported by the Einstein Medical Scientist Training Program.

[3] Additionally supported by National Institutes of Health Biophysics Training Grant T32-GM008572.

[4] To whom correspondence may be addressed: Dept. of Biochemistry, Albert Einstein College of Medicine, 1300 Morris Park Ave., Bronx, NY 10461. Tel: 718-430-8641; E-mail: jon.lai@einstein.yu.edu.

[5] To whom correspondence may be addressed: Dept. of Microbiology and Immunology, Albert Einstein College of Medicine, 1300 Morris Park Ave., Bronx, NY 10461. Tel.: 718-430-8851; E-mail: kartik.chandran@einstein.yu.edu.

[6] The abbreviations used are: EboV, Ebola virus; MarV, Marburg virus; GP, glycoprotein; NHR, N-terminal heptad repeat; CHR, C-terminal heptad repeat; ASLV, avian sarcoma/leukosis virus; rVSV, recombinant vesicular stomatitis virus; eGFP, enhanced green fluorescent protein; mRFP, monomeric red fluorescent protein; m.o.i., multiplicity of infection.

[7] K. Chandran, unpublished data.

triple-stranded coiled coil, projecting the N-terminal fusion peptides into the endosomal membrane. This configuration results in a putative "extended intermediate" conformation in which the entire GP2 ectodomain bridges the viral and host membranes. The three CHRs then fold back and pack into grooves along the NHR core trimer, creating a stable post-fusion "six-helix bundle" configuration. These rearrangements juxtapose the viral and host lipid bilayers, catalyzing their mixing and coalescence, and ultimately lead to delivery of the viral nucleocapsid into the cytoplasm.

The existence of an extended intermediate conformation during membrane fusion by HIV-1 and other prototypic class I envelope glycoproteins was inferred from experiments with synthetic peptides corresponding to the CHR sequence ("C-peptides") (30, 31). C-peptides inhibit membrane fusion and inhibit viral infection by competing with the endogenous CHR for binding to the NHR core trimer of the extended intermediate, thereby arresting the transition to the six-helix bundle. C-peptides with antiviral efficacy *in vitro* and/or *in vivo* have been engineered for many enveloped viruses, including HIV-1 (32), SV5 and Hendra/Nipah paramyxoviruses (33, 34), and severe acute respiratory syndrome coronavirus (35). However, previous attempts to develop such inhibitors for filoviruses based on EboV GP2 yielded peptides with only modest activity (36, 37). Because membrane fusion by filoviruses is thought to occur deep in the endocytic pathway (7, 26, 38), the weak activity of EboV C-peptides may be due to inaccessibility of the extended intermediate. Here, we show that the antiviral activity of an EboV C-peptide is enhanced by conjugation to the arginine-rich segment from HIV-1 Tat protein, which is known to target to endosomes (39, 40). We demonstrate that the activity against EboV and MarV is dependent on this targeting segment and on the endogenous CHR sequence. Mechanistic experiments indicate that the endosome-targeted C-peptide acts on an intermediate in the filovirus entry pathway.

EXPERIMENTAL PROCEDURES

Peptide Synthesis and Purification—All peptides were synthesized by solid-phase peptide synthesis using standard Fmoc (*N*-(9-fluorenyl)methoxycarbonyl) chemistry at the Tufts University Biopolymer Facility. Following synthesis, simultaneous side chain deprotection and cleavage from resin were achieved by treating the resin with 95% trifluoroacetic acid, 2.5% 1,2-ethanedithiol, and 2.5% thioanisole for 3 h. Resin was removed by filtration, and the peptide was precipitated by addition of cold diethyl ether. The peptide was pelleted by centrifugation, washed twice with cold diethyl ether, redissolved in water/acetonitrile, and lyophilized. Crude lyophilized peptides were purified by reverse-phase HPLC on a Vydac C_{18} column (10 μm, 250 × 21.2 mm) with water/acetonitrile mobile phases containing 0.1% trifluoroacetic acid. Peptide purity was generally >95% as judged by analytical reverse-phase HPLC, and the identity of all peptides was confirmed by MALDI-MS (see Table 1). Before the biological studies, the trifluoroacetate counterions were exchanged for chloride ions by dissolving peptides in 50 mM HCl and lyophilizing the resulting solution. (This procedure was performed two to three times for each peptide.) Peptides were dissolved in 10 mM phosphate (pH 7), and the concentration was determined by absorbance at 280 nm (Tat-Ebo, Lys-Ebo, Tat-Scram, Tat, Tat-ASLV, Tat-Ebo^{3S}) or 492 nm (fTat-Ebo and fLys-Ebo).

Cells and Viruses—Grivet (African green monkey) kidney cells (Vero) were maintained at 37 °C and 5% CO_2 with high glucose DMEM (Invitrogen) supplemented with 10% fetal bovine serum. A recombinant vesicular stomatitis Indiana virus (rVSV-GP) encoding the enhanced green fluorescent protein (eGFP) and EboV GP in which the mucin-like domain had been genetically deleted (Δ309–489; Δmuc) was generated and purified as described previously (29). A second recombinant virus (rVSV-G) encoding a monomeric red fluorescent protein fused to the VSV polymerase accessory protein P ((mRFP)-P) in place of the wild-type P protein, was used as a control virus (41). All experiments with rVSVs were performed using enhanced biosafety level 2 procedures approved by the Albert Einstein College of Medicine Institutional Biosafety Committee. VSV pseudotypes expressing eGFP and bearing VSV Indiana G or filovirus GP proteins were generated as described previously (4).

Viral Infectivity Measurements—Infectivity of VSV pseudotypes was measured by manual counting of eGFP- or mRFP-P-positive cells under a fluorescence microscope as described previously (26). Infectivity of rVSVs was measured by fluorescent focus assay as described previously (29). For peptide dose curves, monolayers of Vero cells were pretreated with the indicated concentrations of peptide for 1 h at 37 °C, unless indicated otherwise, and exposed to virus for 1 h at 37 °C. Peptide/virus mixtures were then removed and replaced with fresh growth medium. Viral infectivity was scored as described above.

Confocal Microscopy—Vero cells were plated in 35-mm glass-bottom dishes (MatTek). To prevent escape of the peptide from endosomes and quenching of FITC, cells were treated with 50 mM NH_4Cl for 30 min. Cells were washed with 1 ml of PBS and then treated with 1.5 μM fTat-Ebo or fLys-Ebo for 15 min at 37 °C. The peptide was removed, and the cells were washed extensively with PBS containing 50 mM NH_4Cl. Cells were then incubated with imaging medium (DMEM with no phenol red + 2% FBS) containing 1 μg/ml Hoechst 33342 nuclear stain. Samples were visualized with a Leica SP5 AOBS confocal microscope using a ×63 oil objective. During imaging, cells were maintained at 37 °C in the microscope's environmental chamber. Captured images were converted to the TIFF format using Leica LAS-AF software. Image processing (linear adjustments to brightness and contrast, cropping, and addition of scale bars) was done on the TIFF files using NIH ImageJ. Images were then imported into Illustrator (Adobe Systems) for figure assembly. Endosomal colocalization studies were performed in a similar fashion but with Vero cells that had been transduced with a baculovirus vector encoding mRFP-tagged LAMP1 (CellLight, Invitrogen) at 20 particles/cell. 16 h post-transduction, cells were treated with NH_4Cl and 1.5 μM fTat-Ebo and imaged as described above. Reflectance mode was used to image the cell boundaries, which are depicted as white outlines.

Peptide/Virus Preincubation Experiment—rVSV-GP or rVSV-G was incubated with the desired concentration of pep-

tide in 100 μl of either PBS (pH 7.5) or McIlvaine's citrate-phosphate buffer (pH 5.5) for 1 h at 37 °C. The peptide/virus mixture was then subjected to three serial 10-fold dilutions in growth medium. The diluted mixtures were then added to Vero cell monolayers, and infection was allowed to proceed for 1 h at 37 °C. Viral infectivity was measured as described above. Experiments with cleaved virus were performed in a similar manner except that rVSV-GP was treated with thermolysin (200 μg/ml) for 1 h at 37 °C and then quenched with phosphoramidon (1 mM) prior to addition of the peptide.

Authentic Filovirus Dose Curves—Peptides were diluted to the desired concentration in PBS + Ca^{2+}/Mg^{2+} and added to Vero cells. EboV-eGFP (multiplicity of infection (m.o.i.) = 5 plaque-forming units/cell), EboV-May (m.o.i. = 1 plaque-forming unit/cell), or MarV-Ci67 (m.o.i. = 5 plaque-forming units/cell) was added 1 h later. Viruses were allowed to infect cells for 1 h in the presence of peptide, the inocula were removed, and cells were washed three times with PBS and supplemented with fresh growth medium. Culture supernatants were harvested in TRIzol (Invitrogen) at 48 h post-infection, and virus yield was determined by quantitative real-time PCR (see below). Alternatively, cells were fixed in 10% buffered formalin (Val Tech Diagnostics) for 72 h and stained for quantitative image-based analysis with murine monoclonal antibodies against EboV or MarV GP (6D8 or 9G4 antibody, respectively), followed by Alexa 488-conjugated goat anti-mouse IgG (Invitrogen). All infected cells were stained with Hoechst 33342 and HCS CellMask Red (Invitrogen). Fluorescence images of the stained cells were acquired and analyzed on an Opera QEHS confocal reader (Model 3842, quadruple excitation high sensitivity, PerkinElmer Life Sciences) using a ×10 air objective. Image analysis was accomplished within the Opera environment using standard Acapella scripts. All experiments involving authentic filoviruses were performed under biosafety level 4 conditions at the United States Army Medical Research Institute of Infectious Diseases.

Quantitative Real-time PCR—Total RNA from culture supernatants of untreated cells (mock) or cells infected with EboV or MarV was prepared using the MagMAX 96 RNA extraction kit (Ambion). Quantitative real-time PCR assays were performed on an ABI PRISM 7900HT sequence detection system with an RNA UltraSense one-step kit (Invitrogen) and TaqMan probes (Applied Biosystems) according to the manufacturers' instructions. The final concentrations used in the 20-μl reaction mixture were 5 μl of RNA, 0.4 μM each primer, 0.2 μM probe, 4 μl of 5× reaction mixture, 0.4 μl of ROX, and 1 μl of enzyme mixture. The reaction was run under the following conditions: reverse transcription at 50 °C for 20 min, initial denaturation at 95 °C for 2 min, and amplification for 40 cycles at 95 °C for 15 s and at 60 °C for 30 s. Serial 10-fold dilutions of the assayed virus (10^2–10^7 copies) were used as standards.

RESULTS

Peptide Design—Previous attempts to generate C-peptides against EboV GP resulted in compounds with only weak antiviral activity. Watanabe *et al.* (36) synthesized and tested a peptide corresponding to GP2 residues 610–633 (Fig. 1) and found that large amounts of this peptide were required for modest inhibition of infection by VSV particles bearing VSV-GP. (~1700 μM was needed for ~70% inhibition.) Netter *et al.* (37) observed no inhibition of EboV entry with a peptide corresponding to GP2 residues 610–634 at peptide concentrations up to ~70 μM, but they found that C-peptides derived from the structurally related ASLV Env glycoprotein had potent activity against ASLV entry. Why do similar C-peptides inhibit viral entry mediated by ASLV Env but not by EboV GP? One possible explanation is the limited availability of peptide at the sites of GP-mediated viral membrane fusion. Unlike ASLV Env, which engages the receptor and undergoes initial fusion-related conformational changes at the cell surface (42, 43), EboV GP is likely not triggered until virus particles are deep within the endocytic pathway (7, 26, 38). This model predicts that the antiviral activity of EboV C-peptides could be enhanced by increasing their local concentration in endosomes.

Arginine-rich peptide segments such as those derived from the HIV-1 Tat and *Drosophila melanogaster* Antennapedia proteins have been shown to act as cell-penetrating reagents (39). These peptides are typically employed to deliver cargo to the cytosol and nucleus, but their mode of action involves uptake into and accumulation within endosomes (40). We surmised that conjugation of a Tat-derived Arg-rich sequence to an EboV C-peptide would target the C-peptide to endosomes and increase its access to GP membrane fusion intermediates.

To test this hypothesis, we generated the peptide series shown in Table 1. The peptide Tat-Ebo consists of the HIV-1 Tat Arg-rich sequence appended to residues 610–633 of EboV GP2 by a short Gly-Ser-Gly linker. To explore the contribution of the Tat sequence, a peptide consisting of the Tat sequence alone (Tat-only) and another containing a tetralysine segment in place of the Tat sequence (Lys-Ebo) were also prepared. Previous studies have shown that poly-Lys sequences are much less efficiently internalized than are poly-Arg sequences despite similar cationic charge density (44); therefore, the tetralysine sequence is unlikely to support endosomal delivery of C-peptides. In addition, the tetralysine sequence of Lys-Ebo enhanced the solubility of the C-peptide. Equilibrium analytical ultracentrifugation experiments indicated that peptides comprising residues 610–633 of GP2 alone were prone to aggregation (data not shown). However, we found that both Tat-Ebo and Lys-Ebo were monomeric at micromolar concentrations (see supplemental "Results"). Finally, Tat-Scram and Tat-ASLV, containing a scrambled EboV C-peptide sequence and the ASLV C-peptide sequence, respectively, were generated to test whether inhibitory activity is dependent on the EboV CHR sequence. All peptides were synthesized and purified in good yield using standard methods.

Tat-Ebo Specifically Inhibits VSV-GP Infection in a Tat and CHR Sequence-dependent Manner—We tested the capacity of this peptide series to inhibit infection of Vero cells by rVSV-GP (Fig. 2). We found that Tat-Ebo reduced rVSV-GP infection in a dose-dependent fashion, with ~99% inhibition at the highest concentration tested (75 μM). Cytotoxicity assays indicated that Tat-Ebo was well tolerated by Vero cells in this concentration range (see supplemental "Results"). Importantly, Tat-Ebo had

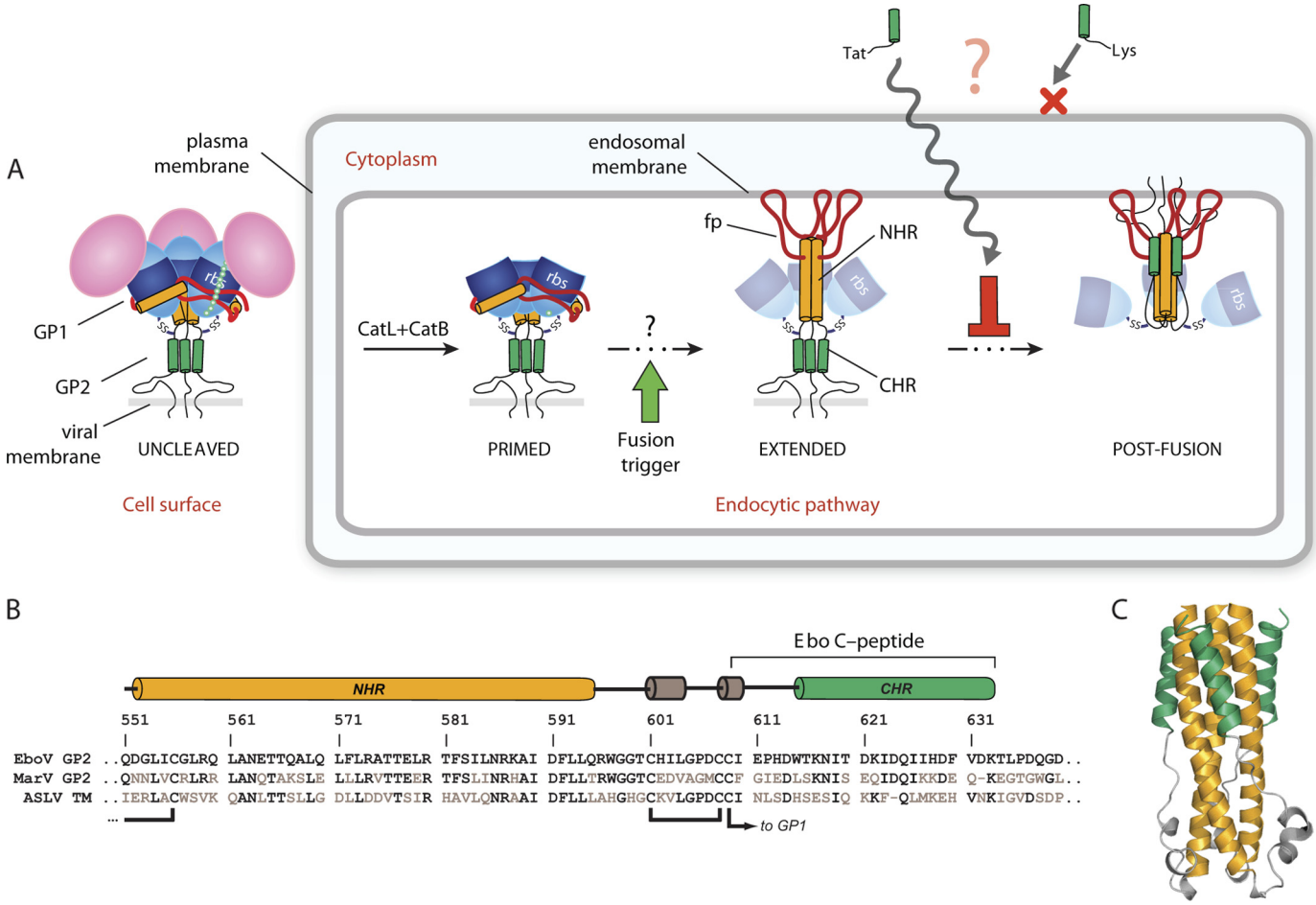

FIGURE 1. *A*, current model for filovirus entry and how this process could be inhibited by an endosome-targeted C-peptide. *CatL*, cathepsin L; *CatB*, cathepsin B; *rbs*, receptor-binding site. *B*, sequence alignment of GP NHR and CHR segments from EboV, MarV, and ASLV. residues that differ from EboV are shown in *gray*. *C*, six-helix bundle structure of the EboV GP2 ectodomain (Protein Data Bank code 2EBO) reported by Malashkevich *et al.* (22).

TABLE 1

Peptides synthesized and tested for activity

The expected ($[MH]^+_{calc}$) and observed ($[MH]^+_{obs}$) monoisotopic masses are shown.

Peptide	Sequence[a]	Charge at pH 7	$[MH]^+_{calc}$	$[MH]^+_{obs}$
Tat-Ebo	YGRKKRRQRRR-GSG-IEPHDWTKNITDKIDQIIHDFVDK	+6	4661.5	4661.9
Lys-Ebo	KKKK-GSG-IEPHDWTKNITDKIDQIIHDFVDK	+2	3633.0	3632.2
Tat-only	YGRKKRRQRRR	+9	1559.0	1558.2
Tat-Scram	YGRKKRRQRRR-GSG-HTEHINFQDDTIKIWPDVIKIKDD	+6	4661.5	4661.8
Tat-ASLV	YGRKKRRQRRR-GSG-FNLSDHSESIQKKFQLMKEHVNKIG	+10	4698.5	4700.2

[a] All peptides were synthesized as C-terminal amides.

no detectable effect on infection by rVSV particles bearing the homologous fusion glycoprotein G, despite the fact that VSV-G also catalyzes viral membrane fusion from within the endocytic pathway in an acid-dependent manner. Therefore, the antiviral activity of Tat-Ebo is specific for EboV GP. Tat-only and Lys-Ebo showed no detectable activity against rVSV-GP, demonstrating that both the localization sequence (Tat) and the C-peptide sequence are required. Tat-Scram and Tat-ASLV also failed to inhibit rVSV-GP infection, providing additional evidence that antiviral activity is specific for EboV GP and indicating that the native CHR sequence is essential. All experiments described here were performed with rVSV-GP lacking the mucin-like domain (Δmuc); however, we found similar inhibition results with Tat-Ebo and rVSV-GP containing the mucin-like domain (see supplemental "Results").

Inhibition of VSV-GP Infection Is Associated with Efficient C-peptide Delivery to Endosomes—To examine the subcellular localization of Tat-Ebo and Lys-Ebo, we generated variants of these peptides bearing an N-terminal FITC moiety (fTat-Ebo and fLys-Ebo, respectively) and exposed them to Vero cells at 37 °C for 15 min. As shown in Fig. 3*A*, fTat-Ebo was taken up into cells and exhibited a punctate pattern characteristic of endosomal distribution. By contrast, fLys-Ebo could not be detected within cells. To confirm that fTat-Ebo accumulated in endosomal compartments, we performed uptake studies with Vero cells expressing mRFP-tagged LAMP1, a protein resident in late endosomes. We found that fTat-Ebo colocalized extensively with LAMP1 (Fig. 3*B*). Therefore, conjugation to the Tat peptide significantly enhances C-peptide uptake into the endocytic pathway.

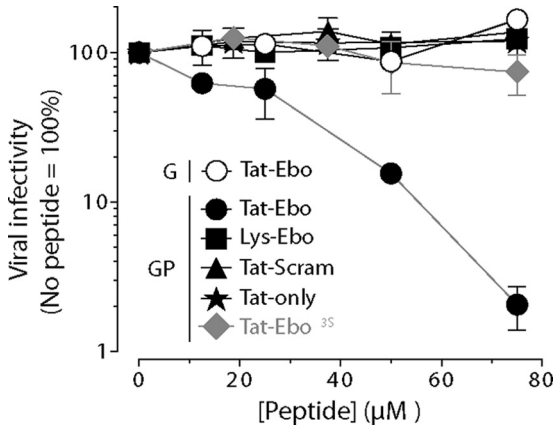

FIGURE 2. **Effect of C-peptides on infection by rVSV-GP and rVSV-G.** Vero cells were pretreated with the indicated concentrations of peptide for 1 h at 37 °C and then exposed to 10-fold serial dilutions of virus. Viral infectivity was determined after 14–16 h by enumeration of fluorescent cells as described under "Experimental Procedures."

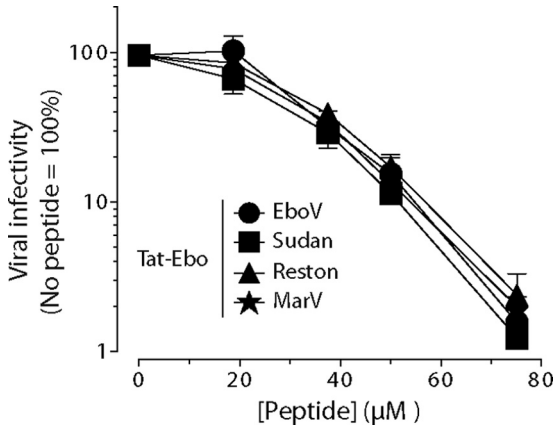

FIGURE 4. **Effect of Tat-Ebo on infection by VSV particles bearing GP proteins derived from three ebolaviruses and one marburgvirus.** Vero cells were pretreated with the indicated concentrations of peptide for 1 h at 37 °C and then exposed to 10-fold serial dilutions of virus. Viral infectivity was determined after 14–16 h as described under "Experimental Procedures."

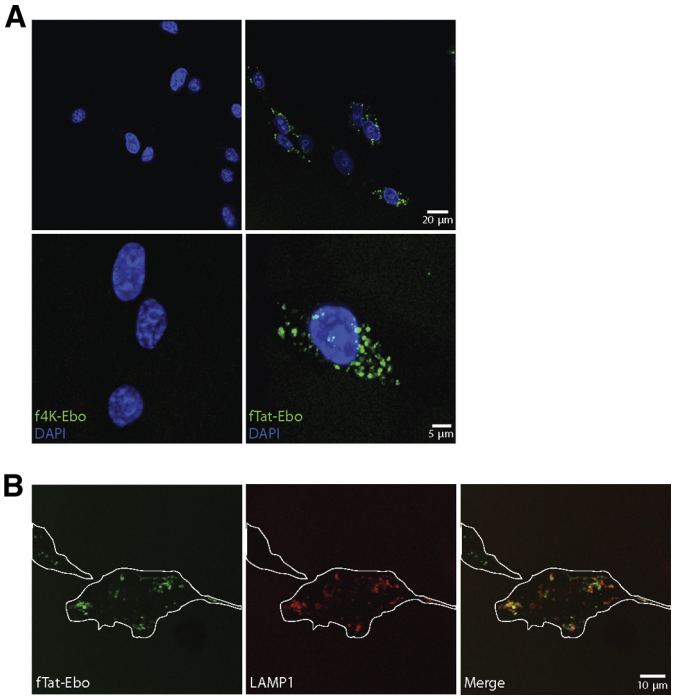

FIGURE 3. *A*, intracellular localization of fTat-Ebo and fLys-Ebo. Vero cells in glass-bottom dishes were pretreated with NH_4Cl to neutralize the endosomal acid pH and then exposed to FITC-labeled peptides for 15 min at 37 °C. Cells were washed, stained with Hoechst 33342, and imaged by confocal fluorescence microscopy. *Left panels*, images were captured with a ×63 objective. *Right panels*, calculated maximal intensity projections are shown. Images were digitally magnified (*upper panel*, ×4; *lower panel*, ×3.2) from images similar to those in the *left panels*. *B*, subcellular localization of internalized fTat-Ebo. Vero cells were transduced with a baculovirus vector encoding mRFP-tagged LAMP1, a late endosome-resident protein, and then treated with fTat-Ebo. LAMP1 and Tat-Ebo were visualized as described for *A*; cells are outlined in *white*. The representative image shown was acquired with a ×63 objective and digitally magnified (×3).

These findings are consistent with our hypothesis that promoting internalization of EboV C-peptides into cells could greatly enhance their antiviral activity.

Tat-Ebo Has Broad Activity against Filovirus GP Proteins—The results in Fig. 2 were obtained with rVSV particles containing EboV GP from the Zaire strain. Because the GP NHR and CHR sequences derived from all ebolaviruses are highly conserved (see Fig. 1), we next considered the possibility that Tat-Ebo also inhibits viral entry mediated by other ebolavirus GP proteins. Accordingly, VSV particles pseudotyped with Sudan or Reston virus GP were generated, and the effect of Tat-Ebo on their infectivity was determined (Fig. 4). We found that Tat-Ebo inhibited both viruses by ~99% at 75 μM. This level of inhibition is comparable with that obtained against the VSV-GP particles containing Zaire virus GP (labeled 'EboV' in Fig. 4). Remarkably, Tat-Ebo also inhibited infection mediated by the more distantly related MarV GP. Therefore, Tat-Ebo is a broad-spectrum inhibitor of infection mediated by filovirus GP proteins.

Tat-Ebo Does Not Act on Extracellular Virus Particles—The filovirus GP-specific activity of Tat-Ebo suggests that this peptide acts at the entry stage to block viral infection. We hypothesized that Tat-Ebo targets the extended intermediate conformation of GP2 during membrane fusion. However, the fusion trigger signal for GP is unknown, and no membrane fusion assays are currently available (25). Therefore, we were unable to directly assess the effect of Tat-Ebo on GP-mediated viral membrane fusion. Nonetheless, we sought to determine whether earlier steps in the viral entry pathway were affected by Tat-Ebo. We first examined the capacity of the peptide to directly inhibit extracellular virus (Fig. 5*A*). rVSV-GP particles were incubated with Tat-Ebo at pH 7.5 or 5.5, and these reaction mixtures were diluted to reduce the concentration of peptide to <1 μM before addition to cells. We found that preincubation of virus particles with high concentrations of peptide at either neutral or acid pH had no detectable effect on viral infection. Therefore, Tat-Ebo is not virucidal and does not negatively affect the pre-fusion conformation of GP in the extracellular space or within acidic endosomes. Similar results were obtained with rVSV-GP that had been treated with thermolysin, which mimics GP proteolytic processing mediated by cathepsin L/cathepsin B, indicating that early intermediates in the entry pathway are also not affected by Tat-Ebo.

To gain further insight, we performed a time-of-addition experiment in which we treated cells with Tat-Ebo for varying lengths of time before or after adding virus (Fig. 5*B*). Maximal

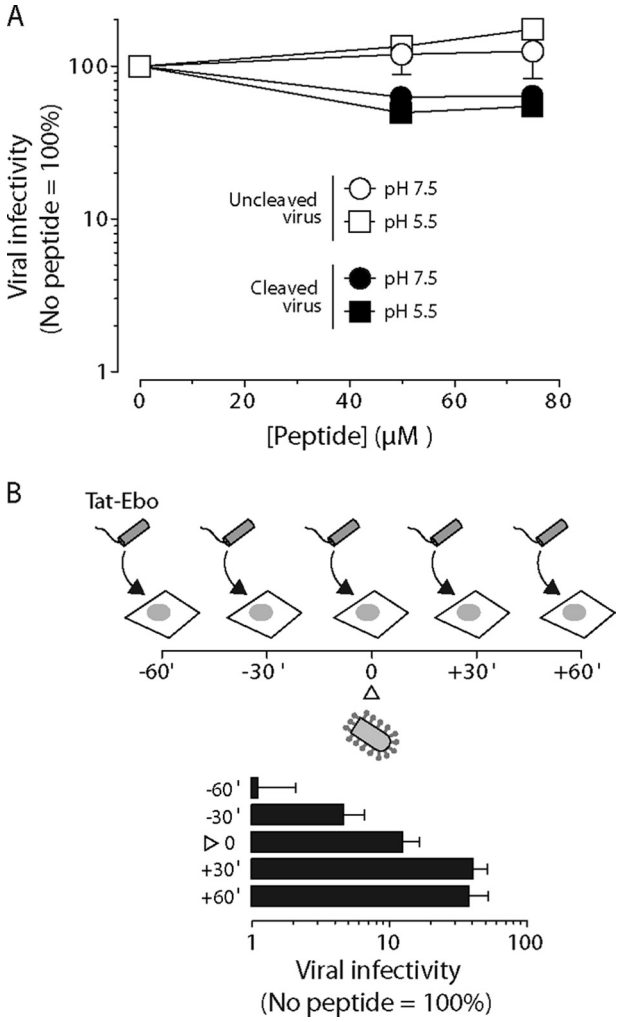

FIGURE 5. **Peptide and virus time-of-addition experiments.** *A*, effect of Tat-Ebo preincubation with virus on infection by rVSV-GP. Virus was incubated with the indicated concentrations of peptide at 37 °C for 1 h at pH 7.5 or 5.5 and then diluted in PBS to reduce the peptide concentration to <1 μM. Diluted peptide/virus mixtures were exposed to Vero cells, and viral infectivity was determined after 14–16 h. *B*, effect of Tat-Ebo time of addition on infection by VSV-GP. As shown in the schematic diagram, Vero cells were incubated with Tat-Ebo (75 μM) for the indicated lengths of time (minutes) before or after addition to virus. At time zero (△), virus and peptide were added together to the cells. After cells were exposed to virus for 1 h at 37 °C, the growth medium was removed and replaced with an agarose medium overlay (see "Experimental Procedures" for details). Viral infectivity was determined after 14–16 h.

inhibition of infection was observed when cells were exposed to peptide for 30–60 min before addition of virus, demonstrating that intracellular accumulation of Tat-Ebo is crucial to its antiviral activity. Moreover, addition of Tat-Ebo to cells 60 min after exposure to virus had little effect on infection, confirming that the peptide blocks cell entry but not later steps in the viral multiplication cycle. Taken together, these findings suggest that Tat-Ebo targets an entry intermediate that exists only within cells.

Hydrophobic Core Positions on the CHR Sequence Are Required for VSV-GP Inhibition by Tat-conjugated C-peptide—We sought to obtain direct evidence that Tat-Ebo targets the EboV GP2 NHR core trimer. Accordingly, we passaged rVSV-GP through eight rounds of growth in the presence of the peptide in an attempt to correlate resistance to Tat-Ebo with mutations in GP2, but this approach failed to identify resistant clones. As an alternative approach, we prepared a variant of Tat-Ebo in which three of the core Ile residues (positions denoted "a" and "d") predicted to contact the NHR core trimer in the EboV GP2 post-fusion six-helix bundle (22, 23) were altered to serine (Tat-Ebo^{3S}, sequence YGRKKRRQRRRGS-GIEPHDWTKN**S**TDK**S**DQ**S**IHDFVDK, where serine residues at the a/d positions are underlined). If interaction with the NHR core trimer is required for inhibition, alteration of the a/d residues in the C-peptide from hydrophobic side chains to polar (serine) side chains should disrupt the contacts with the NHR core trimer and abolish antiviral potency. Indeed, we found that Tat-Ebo^{3S} exhibited no detectable inhibitory activity against rVSV-GP (Fig. 2). These findings suggest that Tat-Ebo directly blocks viral membrane fusion by binding to a GP2 fusion intermediate.

Tat-Ebo Inhibits Infection by Authentic Filoviruses—Although recombinant and pseudotyped VSV particles provide useful systems to study GP-mediated viral entry, observations made in these surrogate systems may not fully reflect the entry pathway used by authentic filoviruses. We therefore tested the capacity of Tat-Ebo, Tat-Ebo^{3S}, and Tat-ASLV to inhibit multiplication by replication-competent EboV and MarV in Vero cells (Fig. 6). After 48 h, Tat-Ebo reduced the numbers of infected cells (≥90% at 50 μM peptide) (Fig. 6*A*) and yields of viral progeny (≥99% at 50 μM peptide) (Fig. 6*B*) for both viruses compared with an untreated control. By contrast, Tat-Ebo^{3S} and Tat-ASLV had no detectable effect. These observations are in full agreement with our findings derived from VSV-GP particles, and they validate the C-peptide endosomal targeting strategy for filoviruses.

DISCUSSION

Enhanced Activity of Endosome-targeted EboV C-peptides—We have demonstrated that the potency of the EboV C-peptide can be enhanced by conjugation to the HIV-1 Tat arginine-rich sequence. The antiviral activity observed at the highest Tat-Ebo concentrations tested here (99% inhibition of infection by authentic filoviruses at 50–75 μM peptide) (Figs. 2, 4, and 6) is ~10-fold higher than that previously reported for a C-peptide lacking the Tat sequence at ~20-fold higher concentrations (36). Furthermore, we have shown that a C-peptide lacking the targeting sequence (Lys-Ebo) is not effective at 75 μM in our hands (Fig. 2). These data are consistent with the work of Netter *et al.* (37), who found that a peptide corresponding to residues 610–634 of EboV GP2 had no activity at ~70 μM. The activity of Tat-Ebo is broad, inhibiting entry and infection by all tested filoviruses to a similar degree (Figs. 2 and 6). Although the concentrations of peptide required to achieve substantial reductions in viral infection and multiplication are too high for Tat-Ebo to be clinically useful, we present here the first evidence that intracellular targeting of a C-peptide can improve activity against a virus that enters via endosomes. This strategy may prove useful against other viruses that fuse from within endosomes and for which inhibitory C-peptides are not available.

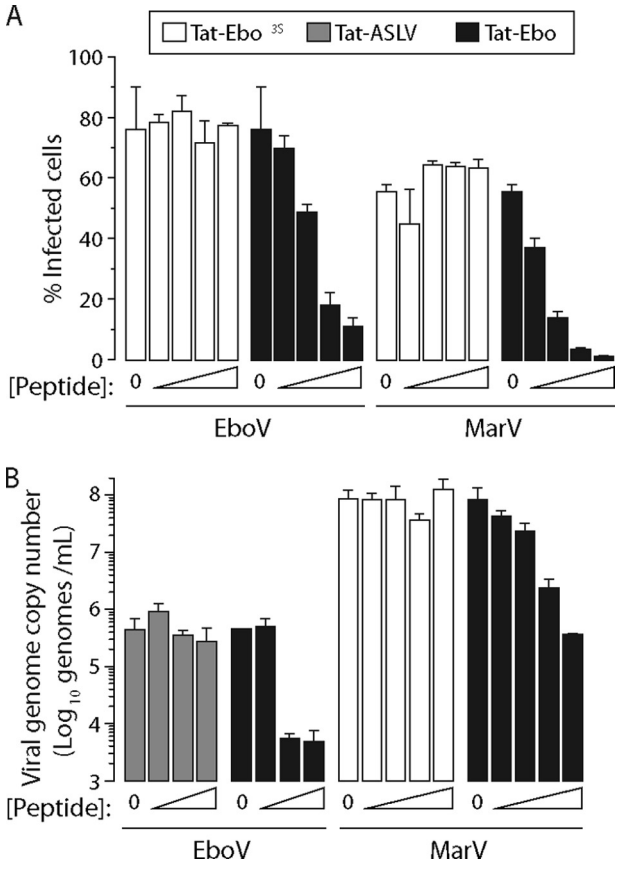

FIGURE 6. **Effect of C-peptides on infection by authentic filoviruses.** *A* and *B*, Vero cells were pretreated with peptide for 1 h at 37 °C and then exposed to EboV or MarV. After 1 h at 37 °C, peptide/virus mixtures were removed, cells were washed, and fresh growth medium was added. Viral infectivity was determined at 48 h as described under "Experimental Procedures." *A*, cells were treated with the indicated peptides at 0, 10, 20, 35, or 50 μM. Percentages of viral antigen-positive infected cells are shown. *B*, cells were treated with 0, 10, 20, 35, or 50 μM Tat-Ebo and Tat-Ebo^{3S} and 0, 10, 50, or 75 μM Tat-ASLV. Viral genome copy numbers determined by quantitative real-time PCR are shown. The m.o.i. was selected for optimal readout: EboV m.o.i. = 1 and MarV m.o.i. = 5.

Mechanism of Inhibition—The specificity of Tat-Ebo activity for filovirus GP2 and the requirement of both the localization signal (Tat) and the native EboV CHR sequence for activity suggest that Tat-Ebo functions by sequestering the extended intermediate and that endosomal accumulation of the peptide is critical for this activity. However, without a direct assay for membrane fusion, we cannot rule out other mechanisms of inhibition. The studies presented here have established that Tat-Ebo does not cause generalized dysfunctions in cellular endocytic pathways (because no effect was observed on VSV-G, which also enters via endosomes) (Fig. 2) and that the peptide does not function by inactivating the virus particle itself (Fig. 5). Furthermore, the anti-filovirus activity of Tat-conjugated C-peptides is dependent on the native CHR sequence (Tat-ASLV is not active) and on maintaining the heptad repeat motif (neither Tat-Scram nor Tat-Ebo^{3S} has detectable activity) (Fig. 2). Tat and other highly cationic peptides have been shown to prevent cell attachment by HSV-1 (45). In cell enzyme-linked immunosorbent assay experiments, we found that Tat-only and Tat-Ebo have similar modest effects on viral attachment to cells (data not shown). However, the fact that Tat-only has no antiviral activity suggests that inhibition of cell attachment is not the major mechanism of inhibition. We also found that uptake of virus-like particles containing EboV GP is affected to some degree by Tat-Ebo but not Tat-only (data not shown). Therefore, it is possible that Tat-Ebo functions by a more complex mechanism that involves early- and late-stage intermediates. Nonetheless, the results presented here demonstrate that Tat-Ebo activity is specific for filovirus GP and that targeting the C-peptide to endosomes is critical for activity.

Targeted Heptad Repeat Peptides as Viral Entry Inhibitors—Several groups have shown that the potency of peptides directed against HIV-1 gp41 can be greatly enhanced by conjugation to agents that localize the peptide to the membrane. Ingallinella *et al.* (46) reported a 15–300-fold activity enhancement (depending upon the HIV-1 strain) for gp41-targeted C-peptides that contain a C-terminal cholesterol moiety, and Wexler-Cohen and Shai (47) demonstrated that HIV-1 N-peptides (corresponding to the NHR) conjugated to cholesterol had potent inhibitory activity. Thorough mechanistic evidence for activity enhancements of conjugated peptides has not been reported. However, the location of the cholesterol moiety has a strong influence on activity: those peptides containing cholesterol at the C terminus were much more potent than peptides containing cholesterol at the N terminus (47). Because the six-helix bundle structure of the gp41 ectodomain contains antiparallels CHR and NHR helices and because the extended intermediate is postulated to have the N terminus of the NHR near the viral membrane, it has been proposed that the method of enhanced activity for the cholesterol-conjugated peptides involves localization and fixing the orientation of the CHR segment to bind the NHR core trimer (47). Inclusion of the cholesterol moiety increases the local concentration of the C-peptide such that it is primed for binding to the NHR core trimer during generation of the transient extended intermediate. Similar strategies have recently been used to inhibit paramyxoviruses (48), and this membrane-targeting strategy may be useful in other virus systems. The work described here has demonstrated that targeting C-peptides to endosomal compartments can serve as a parallel approach to localize inhibitors to sites of membrane fusion.

Acknowledgments—We thank Michael Brenowitz (Albert Einstein College of Medicine) for assistance with analytical ultracentrifugation studies and Betsy Herold, Margaret Kielian, Vinayaka Prasad, and Sean Whelan for helpful discussions.

REFERENCES

1. Kuhn, J. H., Becker, S., Ebihara, H., Geisbert, T. W., Johnson, K. M., Kawaoka, Y., Lipkin, W. I., Negredo, A. I., Netesov, S. V., Nichol, S. T., Palacios, G., Peters, C. J., Tenorio, A., Volchkov, V. E., and Jahrling, P. B. (2010) *Arch. Virol.* **155,** 2083–2103
2. Kuhn, J. H. (2008) *Arch. Virol. Suppl.* **20,** 13–360
3. Feldmann, H., and Geisbert, T. W. (2011) *Lancet* **377,** 849–862
4. Takada, A., Robison, C., Goto, H., Sanchez, A., Murti, K. G., Whitt, M. A., and Kawaoka, Y. (1997) *Proc. Natl. Acad. Sci. U.S.A.* **94,** 14764–14769
5. Wool-Lewis, R. J., and Bates, P. (1998) *J. Virol.* **72,** 3155–3160
6. Jeffers, S. A., Sanders, D. A., and Sanchez, A. (2002) *J. Virol.* **76,** 12463–12472
7. Lee, J. E., Fusco, M. L., Hessell, A. J., Oswald, W. B., Burton, D. R., and

Saphire, E. O. (2008) *Nature* **454,** 177–182
8. Volchkov, V. E., Feldmann, H., Volchkova, V. A., and Klenk, H. D. (1998) *Proc. Natl. Acad. Sci. U.S.A.* **95,** 5762–5767
9. Wool-Lewis, R. J., and Bates, P. (1999) *J. Virol.* **73,** 1419–1426
10. Manicassamy, B., Wang, J., Jiang, H., and Rong, L. (2005) *J. Virol.* **79,** 4793–4805
11. Dube, D., Brecher, M. B., Delos, S. E., Rose, S. C., Park, E. W., Schornberg, K. L., Kuhn, J. H., and White, J. M. (2009) *J. Virol.* **83,** 2883–2891
12. Brindley, M. A., Hughes, L., Ruiz, A., McCray, P. B., Jr., Sanchez, A., Sanders, D. A., and Maury, W. (2007) *J. Virol.* **81,** 7702–7709
13. Kuhn, J. H., Radoshitzky, S. R., Guth, A. C., Warfield, K. L., Li, W., Vincent, M. J., Towner, J. S., Nichol, S. T., Bavari, S., Choe, H., Aman, M. J., and Farzan, M. (2006) *J. Biol. Chem.* **281,** 15951–15958
14. Lin, G., Simmons, G., Pöhlmann, S., Baribaud, F., Ni, H., Leslie, G. J., Haggarty, B. S., Bates, P., Weissman, D., Hoxie, J. A., and Doms, R. W. (2003) *J. Virol.* **77,** 1337–1346
15. Takada, A., Fujioka, K., Tsuiji, M., Morikawa, A., Higashi, N., Ebihara, H., Kobasa, D., Feldmann, H., Irimura, T., and Kawaoka, Y. (2004) *J. Virol.* **78,** 2943–2947
16. Kaletsky, R. L., Simmons, G., and Bates, P. (2007) *J. Virol.* **81,** 13378–13384
17. Harrison, S. C. (2008) *Nat. Struct. Mol. Biol.* **15,** 690–698
18. White, J. M., Delos, S. E., Brecher, M., and Schornberg, K. (2008) *Crit. Rev. Biochem. Mol. Biol.* **43,** 189–219
19. Eckert, D. M., and Kim, P. S. (2001) *Annu. Rev. Biochem.* **70,** 777–810
20. Earp, L. J., Delos, S. E., Park, H. E., and White, J. M. (2005) *Curr. Top. Microbiol. Immunol.* **285,** 25–66
21. Ito, H., Watanabe, S., Sanchez, A., Whitt, M. A., and Kawaoka, Y. (1999) *J. Virol.* **73,** 8907–8912
22. Malashkevich, V. N., Schneider, B. J., McNally, M. L., Milhollen, M. A., Pang, J. X., and Kim, P. S. (1999) *Proc. Natl. Acad. Sci. U.S.A.* **96,** 2662–2667
23. Weissenhorn, W., Carfí, A., Lee, K. H., Skehel, J. J., and Wiley, D. C. (1998) *Mol. Cell* **2,** 605–616
24. Gallaher, W. R. (1996) *Cell* **85,** 477–478
25. Lee, J. E., and Saphire, E. O. (2009) *Future Virol.* **4,** 621–635
26. Chandran, K., Sullivan, N. J., Felbor, U., Whelan, S. P., and Cunningham, J. M. (2005) *Science* **308,** 1643–1645
27. Schornberg, K., Matsuyama, S., Kabsch, K., Delos, S., Bouton, A., and White, J. (2006) *J. Virol.* **80,** 4174–4178
28. Hood, C. L., Abraham, J., Boyington, J. C., Leung, K., Kwong, P. D., and Nabel, G. J. *J. Virol.* **84,** 2972–2982
29. Wong, A. C., Sandesara, R. G., Mulherkar, N., Whelan, S. P., and Chandran, K. (2010) *J. Virol.* **84,** 163–175
30. Chan, D. C., Chutkowski, C. T., and Kim, P. S. (1998) *Proc. Natl. Acad. Sci. U.S.A.* **95,** 15613–15617
31. Furuta, R. A., Wild, C. T., Weng, Y., and Weiss, C. D. (1998) *Nat. Struct. Biol.* **5,** 276–279
32. Wild, C. T., Shugars, D. C., Greenwell, T. K., McDanal, C. B., and Matthews, T. J. (1994) *Proc. Natl. Acad. Sci. U.S.A.* **91,** 9770–9774
33. Russell, C. J., Jardetzky, T. S., and Lamb, R. A. (2001) *EMBO J.* **20,** 4024–4034
34. Porotto, M., Rockx, B., Yokoyama, C. C., Talekar, A., Devito, I., Palermo, L. M., Liu, J., Cortese, R., Lu, M., Feldmann, H., Pessi, A., and Moscona, A. (2010) *PLoS Pathog.* **6,** e1001168
35. Ujike, M., Nishikawa, H., Otaka, A., Yamamoto, N., Yamamoto, N., Matsuoka, M., Kodama, E., Fujii, N., and Taguchi, F. (2008) *J. Virol.* **82,** 588–592
36. Watanabe, S., Takada, A., Watanabe, T., Ito, H., Kida, H., and Kawaoka, Y. (2000) *J. Virol.* **74,** 10194–10201
37. Netter, R. C., Amberg, S. M., Balliet, J. W., Biscone, M. J., Vermeulen, A., Earp, L. J., White, J. M., and Bates, P. (2004) *J. Virol.* **78,** 13430–13439
38. Saeed, M. F., Kolokoltsov, A. A., Albrecht, T., and Davey, R. A. (2010) *PLoS Pathog.* **6,** e1001110
39. Gump, J. M., and Dowdy, S. F. (2007) *Trends Mol. Med.* **13,** 443–448
40. Richard, J. P., Melikov, K., Brooks, H., Prevot, P., Lebleu, B., and Chernomordik, L. V. (2005) *J. Biol. Chem.* **280,** 15300–15306
41. Heinrich, B. S., Cureton, D. K., Rahmeh, A. A., and Whelan, S. P. (2010) *PLoS Pathog.* **6,** e1000958
42. Earp, L. J., Delos, S. E., Netter, R. C., Bates, P., and White, J. M. (2003) *J. Virol.* **77,** 3058–3066
43. Smith, J. G., Mothes, W., Blacklow, S. C., and Cunningham, J. M. (2004) *J. Virol.* **78,** 1403–1410
44. Mitchell, D. J., Kim, D. T., Steinman, L., Fathman, C. G., and Rothbard, J. B. (2000) *J. Pept. Res.* **56,** 318–325
45. Akkarawongsa, R., Potocky, T. B., English, E. P., Gellman, S. H., and Brandt, C. R. (2008) *Antimicrob. Agents Chemother.* **52,** 2120–2129
46. Ingallinella, P., Bianchi, E., Ladwa, N. A., Wang, Y. J., Hrin, R., Veneziano, M., Bonelli, F., Ketas, T. J., Moore, J. P., Miller, M. D., and Pessi, A. (2009) *Proc. Natl. Acad. Sci. U.S.A.* **106,** 5801–5806
47. Wexler-Cohen, Y., and Shai, Y. (2009) *PLoS Pathog.* **5,** e1000509
48. Porotto, M., Yokoyama, C. C., Palermo, L. M., Mungall, B., Aljofan, M., Cortese, R., Pessi, A., and Moscona, A. (2010) *J. Virol.* **84,** 6760–6768